Pathogenic rickettsiae utilize the phosphatidylserine binding receptor CD300f on macrophages for host invasion and pathogenesis.

Author information

Oliver H. Voss*, Imran Moin, Hodalis Gaytan, Saif Ullah, Mohammad Sadik, Abdu F. Azad, and M. Sayeedur Rahman

Department of Microbiology and Immunology, University of Maryland School of Medicine, Baltimore, MD 21201, USA

*Correspondence: ovoss@som.umaryland.edu (O.H.V.)

ORCIDs:

Oliver H. Voss: 0000-0002-1436-2809

M. Sayeedur Rahman: 0000-0002-9216-9270

Abdu F. Azad: 0000-0003-1535-6395

Keywords: *R. typhi*, *R. rickettsii*, CD300f, phosphatidylserine, phagocytosis, macrophages, bacterial host dissemination

Author Contributions

O.H.V., M.S.R., and A.F.A. planned the research, analyzed, and interpreted the data; O.H.V., I.M., H.G., M.S., S.U., and M.S.R. performed the experiments; A.F.A., and O.H.V., contributed to the overall project administration and supervision; O.H.V., M.S.R., and A.F.A. wrote the manuscript; and all authors participated in editing the manuscript.

Abstract

Some arthropod-borne obligate intracellular rickettsiae are among the most virulent human pathogens. Upon entry, *Rickettsia* species modulate immune (e.g., macrophages; MΦ) and non-immune cell (e.g., endothelial cells) responses to create a habitable environment for host colonization. In particular, MΦ play a crucial role in either terminating an infection at an early stage or succumbing to bacterial replication and colonization. However, our understanding on how *Rickettsia* species modulate crucial cellular processes within MΦ, including phagocytosis, and host cell defenses, to establish an intracytosolic replication niche, remain poorly defined. In this study, we describe a previously unappreciated mechanism, in which pathogenic rickettsiae infection is mediated by the phosphatidylserine (PS)-binding receptor, CD300f. We found that CD300f$^{-/-}$ mice but not wild-type (WT) C57BL/6J mice were protected against *R. typhi*- or *R. rickettsii* [*Shelia Smith*]-induced fatal rickettsiosis. Adoptative transfer studies further revealed that CD300f-expressing bone marrow-derived macrophages (BMDMΦ) are important mediators to control rickettsiosis in WT mice. Mechanistical analysis, using WT or CD300f$^{-/-}$ BMDMΦ, showed that CD300f facilitates the engulfment of both pathogenic *R. typhi* and *R. rickettsii* species, likely via a PS-mediated mechanism. Furthermore, CD300f was involved in the intracytosolic replication of both pathogenic rickettsiae by differentially modulating the anti-inflammatory Interleukin (IL)-10 and anti-rickettsial IL-1α and IL-1β cytokine responses. Collectively, our findings describe a previously unappreciated role for the efferocytic receptor, CD300f, to facilitate engulfment and the intracellular survival of pathogenic rickettsiae within the host.

Significance Statement

Vector-borne diseases, which are transmitted by hematophagous arthropods, like ticks and fleas, present a perilous threat to public health. In fact, tick- and flea-borne rickettsial diseases are on the rise globally and our current inadequate understanding on how *Rickettsia* interacts with their mammalian host has significantly impaired the development of effective interventions against pathogenic rickettsial infections. Here, we identified the phosphatidylserine (PS)-receptor, CD300f, as an important mediator of pathogenic rickettsiae infection *in vivo* and *in vitro*. Specifically, we showed that CD300f-expressing macrophages facilitate rickettsial infection by differentially modulating anti-inflammatory Interleukin (IL)-10 and anti-rickettsial IL-1α and IL-1β

61 cytokine responses. In sum, our data described CD300f as an important regulator of rickettsial infection and
62 may present a target for therapeutic intervention.
63
64 **Introduction**
65 Vector-borne diseases represent a serious concern for global public health. In the United States, many
66 vector-borne pathogens, transmitted by hematophagous arthropods (e.g., ticks and fleas), are on the rise, as
67 exemplified by recent outbreaks of *R. rickettsii*, an etiologic agent of Rocky Mountain Spotted Fever, in Arizona
68 (1) and of *R. typhi*, an etiologic agent of murine typhus, in California (2) and in Texas (3). Human infection with
69 rickettsiae occurs via infected arthropods (e.g., ticks and fleas) either through their bite or deposited infected
70 feces into host's dermis and mucosal surfaces. Upon entry, *Rickettsia* species (spp) encounter tissue-resident
71 immune cells, like macrophages (MΦ) and dendritic cells (4). MΦ play a crucial role in either terminating an
72 infection at an early stage of host invasion, which commonly is the fate of non-pathogenic *Rickettsia* spp, or
73 succumbing to bacterial replication and pathogen colonization as well as host dissemination to distant organs
74 (4). However, the key cellular processes of rickettsial obligate lifestyle, which includes ***I)*** internalization by
75 phagocytosis (into professional phagocytes, like MΦ) or by induced phagocytosis (into main target endothelial
76 cells), ***II)*** regulation of membrane dynamics and intracellular trafficking, and ***III)*** evasion of host defenses to
77 establish an intracytosolic replication niche, remain poorly defined and have impaired the development of
78 effective interventions against pathogenic rickettsiae (4, 5). Specifically, our understanding on rickettsiae-
79 induced phagocytosis relies mostly on reports from endothelial cells, leaving the mechanism of engulfment of
80 rickettsiae by host defense cells, like MΦ, widely unexplored. In fact, preceding research on endothelial cells
81 has revealed the identity of four host receptors Ku70 (6), α2β1 (7), FGFR1 (8), Epac1 (9), with limited effects
82 on *Rickettsia* invasion (~ 40%) when silenced individually, supporting the hypothesis of an alternative receptor
83 (on host)-ligand (on rickettsiae) system for rickettsial engulfment. Yet the precise mechanism(s) remain to be
84 elucidated.
85 Phagocytosis of apoptotic cells (AC) by MΦ [aka efferocytosis], is critical for maintaining homeostasis
86 by removing ACs before becoming proinflammatory and immunogenic causing autoimmune diseases (10, 11).
87 Importantly, the same mechanism can also be hijacked by various pathogens, including viruses and bacteria,
88 to promote host cell invasion (12). In fact, pathogens have been shown to exploit efferocytosis through

89 externalization of “eat-me” signals [e.g., phosphatidylserine (PS)] to gain access to various PS-binding
90 receptors on MΦ, including CD300s (12, 13) to evade host immune surveillance, and to promote their
91 dissemination within the host (12). The CD300 family are type I transmembrane cell surface receptors with a
92 single immunoglobulin (Ig)V-like extracellular domain that can transmit either activating or inhibitory signals
93 (11, 14, 15). Specifically, activating receptors have usually short intracellular tails and gain activation potential
94 through binding of adaptor molecules (e.g., DAP12) harboring immunoreceptor tyrosine-based activation
95 motifs. In contrast, inhibitory receptors have immunoreceptor tyrosine-based inhibitory motifs within their
96 intracellular tails. The orthologous mouse family has a variety of names, including CMRF-like molecules (CLM)
97 (15), but for simplicity, herein, we use the human nomenclature for both species. CD300f is predominantly
98 expressed by myeloid cells and is unique as it displays both activating and inhibitory signaling capabilities (11,
99 15). Moreover, CD300f is a PS-binding receptors, which regulates efferocytosis in professional phagocytes
100 (e.g., MΦ) (11, 15–19). In line with such unique role CD300f has also been shown to play an important role in
101 modulating allergic, inflammatory, autoimmune viral and bacterial responses. However, the contributing role of
102 PS-binding receptor CD300f during rickettsiae engulfment in MΦ (or other immune defense cells) causing
103 ultimately fatal rickettsiosis has not been investigated.

104 Here, we assessed the functional role of CD300f in rickettsial pathogenesis, by taking advantage of a
105 well-accepted *CD300f* knockout mouse model (17). Our studies demonstrate, using our previously established
106 mouse model of fatal rickettsiosis (20), that CD300f$^{-/-}$ mice, but not wild-type (WT) C57BL/6J mice were
107 protected against *R. typhi*- or *R. rickettsii* [*Shelia Smith*]-induced lethality. Adoptative transfer studies identified
108 CD300f-expressing bone marrow-derived macrophages (BMDMΦ) as critical mediators in controlling rickettsial
109 infection in mice. Further mechanistical analysis showed that CD300f facilitates the engulfment of *R. typhi* and
110 *R. rickettsii* into BMDMΦ, likely via PS-dependent mechanism. In addition, our data suggest the survival
111 advantage of *R. typhi* and *R. rickettsii* within WT BMDMΦ is due to a CD300f-mediated increase in the
112 expression of anti-inflammatory IL-10 levels and the decrease in anti-rickettsial IL-1α and IL-1β cytokine
113 responses. Collectively, our findings describe a previously unappreciated role for CD300f during rickettsial
114 infection.

115

116 **Results**

117 **CD300f exacerbates the pathogenesis of rickettsiae.**

118 Efferocytosis carried out by professional phagocytes (e.g., MΦ) is critical for maintaining cellular
119 homeostasis by removing large quantities of ACs before they become proinflammatory and immunogenic
120 causing the development of autoimmune diseases (10–12). Importantly, the same mechanism can also be
121 hijacked by viruses and bacteria to promote their host invasion (12, 13). In fact, both kind of pathogens utilize
122 PS externalization to gain access to PS-receptors, including Tyro3, Axl, MerTK, TIM1/4, or CD300s (e.g.,
123 CD300f) (12, 13). As a result, we undertook experiments to investigate, how pathogenic *Rickettsia* exploit
124 efferocytic receptor-mechanisms to invade and colonize the host and initiate disease. We tested the *in vivo*
125 role for CD300f in *Rickettsia* colonization by employing our established C57BL/6J wild-type (WT) mouse model
126 of severe (~LD_{50}) rickettsiosis using both pathogenic *R. typhi* or *R. rickettsii* spp (20). As shown previously, we
127 observed a mortality rate of ~50% in WT mice using *R. typhi* (~68 hpi) and *R. rickettsii* (~50 hpi) (Figs. 1A and
128 1C). Our findings further showed that, *R. typhi*- or *R. rickettsii*-infected CD300f$^{-/-}$ mice, but not WT mice,
129 showed no signs of lethality during infection (Figs. 1A and 1C). Bacterial burden in spleens from both
130 *Rickettsia* spp infected WT and CD300f$^{-/-}$ mice confirmed successful infection at day 3 post-infection.
131 Furthermore, *R. typhi*- and *R. rickettsii*-infected WT mice displayed a significantly higher bacterial burden in the
132 spleens as compared to that from both *Rickettsia* spp infected CD300f$^{-/-}$ mice at day 3 and 7 (Figs. 1B and 1D).
133 This correlated with the observed differences in the spleen sizes and weights of the infected animals (Fig. S1).
134 In sum, these data suggest that presence of CD300f exacerbates rickettsiosis *in vivo*.
135

136 **Macrophages are crucial mediators of *R. typhi* and *R. rickettsii* infection *in vivo*.**

137 Given the findings from others and our laboratory highlighting the importance of MΦ during rickettsiae
138 infection, we wanted to explore the role of MΦ in modulating the susceptibility differences between CD300f$^{-/-}$
139 and WT mice during *R. typhi* and *R. rickettsii* infection. As such, we first injected C57/B6J WT and CD300f$^{-/-}$-
140 deficient mice via tail vein (*i.v.*) with liposome-encapsulated phosphate-buffered saline (PBS)- or
141 dichloromethylene biphosphate (Cl_2MBP) at 48 and 24 hrs to deplete endogenous MΦ as described previously
142 (18, 20). Next, mice were infected with a lower dose (10^5 PFU) of either *R. typhi* or *R. rickettsii* that resulted in
143 a ~LD_{25} in WT mice, which agrees with our previous findings (20) (Fig. 2A). Our data further showed that
144 depletion of MΦ not only enhanced the mortality rate of *R. typhi*- and *R. rickettsii*-infected WT mice but also
145 impaired the survival advantage observed in CD300f$^{-/-}$ mice (Figs. 2B & 2D). In contrast, injection of PBS-

146 liposomes did not alter the mortality rate of *R. typhi*- or *R. rickettsii*-infected WT or CD300f$^{-/-}$ mice (Figs. 2B &
147 2D). Of note, development of splenomegaly and consequently bacterial loads within the spleens was
148 significantly increased in rickettsiae-infected Cl_2MBP-treated mice as compared to bacteria-infected PBS-
149 liposomes treated WT and CD300f$^{-/-}$ animals (Fig. S2, Figs. 2C & 2E). Taken together our findings suggest that
150 the presence of CD300f on MΦ plays a key role in rickettsial infection.
151
152 **CD300f on macrophages contributes to *R. typhi* and *R. rickettsii* infection *in vivo*.**
153 To further assess the role of CD300f-expressing MΦ in modulating rickettsiosis *in vivo*, we next injected
154 WT mice via tail vein (*i.v.*) with PBS- or Cl_2MBP-liposome at 72 and 48 hrs prior to injections with bone marrow
155 derived MΦ (BMDMΦ) purified from either CD300f$^{-/-}$, or WT mice at a concentration of 5 x 10^6 cells per mouse
156 (Fig. 3A). Twenty-four hours later, mice were injected (*i.v.*) with either *R. typhi* or *R. rickettsii* [10^5 PFU] (Figs.
157 3B & 3D), similar to infection models of mild rickettsiosis as described previously (20). Our data showed that
158 removal of MΦ not only enhanced the mortality rate of both *R. typhi*- and *R. rickettsii*-infected WT mice but also
159 showed that adoptively transferred BMDMΦ from WT mice partially rescued fatal rickettsiosis in Cl_2MBP-
160 treated WT mice (Figs. 3B & 3D). Importantly, injection of BMDMΦ from CD300f$^{-/-}$ mice into Cl_2MBP-treated
161 WT mice further reduced the mortality rate of *R. typhi*- or *R. rickettsii*-infected WT mice to levels seen in
162 bacterial-infected PBS-liposomes treated WT mice (Figs. 3B & 3D). In line with our findings, the development
163 of splenomegaly and bacterial loads within the spleens was significantly increased in Cl_2MBP-treated WT mice
164 as compared to PBS-liposomes treated WT mice (Fig. S3, Figs. 3C & 3E). Moreover, adoptive transfer of WT
165 BMDMΦ reduced the bacterial burden in rickettsiae-infected Cl_2MBP-treated WT mice (Figs. 3C & 3E).
166 Importantly, injection of BMDMΦ from CD300f$^{-/-}$ mice further reduced the bacterial burden in Cl_2MBP-treated
167 WT mice, reaching close to the levels observed in rickettsiae-infected PBS-liposomes treated WT mice (Figs.
168 3C & 3E). Collectively, these data showed that CD300f-expressing MΦ are crucial in modulating host invasion
169 by pathogenic *Rickettsia* from both SFG and TGs.
170
171 **CD300f, but no other member of CD300 family contributes to *R. typhi*- or *R. rickettsii* infection in**
172 **macrophages.**

173 As iterated above, MΦ are one of the cell types first encountered by rickettsiae at the site of infection
174 and are considered key players to either terminate the infection early at the skin site or allow initial pathogen
175 colonization and subsequent dissemination within the host (4). In fact, our recent findings showed that
176 pathogenic rickettsiae modulate inflammasome- and autophagy-dependent responses in MΦ to facilitate
177 replication within the host (20, 21). As data shown above revealed that CD300f-expressing MΦ play an
178 important role in host invasion by pathogenic *Rickettsia* spp, we further evaluated if any other CD300 family
179 member contributes to bacterial infection into host. We focused on family members that function as activating
180 receptors promoting efferocytosis by MΦ (e.g., CD300d, or others)(11, 15, 17, 18, 22). In this effort, we
181 assessed the phagocytic capability of purified BMDMΦ from WT, CD300d$^{-/-}$ or CD300f$^{-/-}$ mice, to engulf *R. typhi*
182 or *R. rickettsii* by immunofluorescent assay (IFA). Our data showed that, unlike WT or CD300d$^{-/-}$ BMDMΦ,
183 phagocytosis of both *R. typhi* and *R. rickettsii* was significantly reduced in CD300f$^{-/-}$ BMDMΦ (Fig. 4A). To
184 further confirm these findings, we employed qRT-PCR and found similar results (Fig. 4B). These data indicate
185 that CD300f, but not CD300d, contributed to the engulfment of *R. typhi* and *R. rickettsii* into MΦ. As CD300f
186 primarily functions as a PS-binding receptors to regulate efferocytosis (11, 16–19, 22), we further determined
187 whether CD300f-mediated engulfment of pathogenic rickettsiae by MΦ involves PS. This was achieved by
188 using purified *R. typhi* and *R. rickettsii* incubated with increasing concentrations of recombinant Annexin V
189 (rAnxV), a molecule known to block PS-mediated efferocytosis (16, 17, 22), and then utilized to infect WT
190 BMDMΦ. To distinguish adherent from engulfed bacteria, rickettsial engulfment was determined by differential
191 staining for IFA as described previously (20, 23). Our findings showed that pretreatment with rAnxV inhibited
192 the engulfment of both pathogenic rickettsiae in a dose-dependent manner (Figs. S4A & S4B). In addition,
193 experiments using heat-inactivated (HI) rAnxV were employed as specificity control and failed to inhibit
194 bacteria uptake (Figs. S4A & S4B), indicating that PS is likely a ligand contributing to *R. typhi* or *R. rickettsii*
195 invasion of MΦ. Engagement of the PS-CD300f-mechanism is commonly linked to an anti-inflammatory
196 cytokine response (11, 16–19, 22). Intriguingly, we recently showed that the intracellular survival of pathogenic
197 rickettsiae involved in the downregulations of pro-inflammatory cytokine responses, including IL-1α and IL-
198 1β (20).

199 To gain further mechanistic insight, we evaluated the anti-inflammatory IL-10 and pro-inflammatory IL-
200 1β and IL-1α cytokine responses in cultured supernatants of *R. typhi*- and *R. rickettsii*-infected WT BMDMΦ, as

201 well as CD300f$^{-/-}$ BMDMΦ. We observed that infection of WT BMDMΦ with *R. typhi* or *R. rickettsii* produced
202 significantly lower levels of IL-1β or IL-1α cytokine, while infection of CD300f$^{-/-}$ BMDMΦ resulted in an increase
203 of IL-1β or IL-1α cytokine levels (Fig. 4C). Furthermore, we found that *R. typhi*- or *R. rickettsii*-infected WT
204 BMDMΦ produced significantly higher levels of IL-10, as compared to infection of CD300f$^{-/-}$ BMDMΦ with
205 pathogenic rickettsiae (Fig. 4C). Given these data, we sought to determine the biological importance of
206 CD300f-dependent modulation of IL-1β or IL-1α cytokine responses in restricting the survival of both
207 pathogenic rickettsiae in MΦ. In this effort, we neutralized the activity of IL-1β or IL-1α cytokines using anti-IL-
208 1β or anti-IL-1α antibodies and assessed the effect on the bacterial burdens for *R. typhi*-, and *R. rickettsii*-
209 infected WT or CD300f$^{-/-}$ BMDMΦ. Neutralization of IL-1α or IL-1β (with a lower effectiveness) resulted in an
210 increase in bacterial loads of *R. typhi*-, or *R. rickettsii*-infected WT BMDMΦ (Figs. 4D & 4E). Importantly,
211 antibody neutralization of IL-1α or IL-1β (with a lower effectiveness), increased the bacterial burdens of *R.*
212 *typhi*-, and *R. rickettsii*-infected CD300f$^{-/-}$ BMDMΦ, reaching the levels similar to that observed in infected WT
213 BMDMΦ (Figs. 4D & 4E). Of note, concurrent anti-IL-1β and anti-IL-1α antibody treatments in *R. typhi*- and *R.*
214 *rickettsii*-infected WT or CD300f$^{-/-}$ BMDMΦ did not result in a synergistic effect (Figs. 4D & 4E). The efficiency
215 of antibody-mediated blocking was validated by comparing the levels of IL-1α or IL-1β cytokines in the
216 supernatants of IgG isotype control, IL-1α or IL-1β antibody-treated Rickettsia-infected WT BMDMΦ, as well as
217 CD300f$^{-/-}$ BMDMΦ (Fig. S5). Collectively, our data present a previously unappreciated pathway by which
218 pathogenic rickettsiae engage the efferocytic receptor, CD300f, on MΦ to support their host invasion.
219

220 **Discussion**

221 Successful host invasion by intracellular bacteria requires receptor-ligand engagement and subversion of
222 host endocytic bactericidal pathways (24, 25). However, research on how *Rickettsia* spp invade, and avoid
223 cytosolic defense surveillance for host colonization is only now emerging beyond the difficulties posed by their
224 obligate intracellular replication and a life cycle that involves arthropod and vertebrate hosts (4, 5). In fact,
225 research focused on characterizing *Rickettsia*-specific immunodominant outer membrane proteins [e.g.,
226 surface cell antigens (Scas)] or ligands, like lipopolysaccharides (LPS) failed to show a significant impact on
227 the virulence in mammalian host systems (26, 27). One possible explanation for these failed approaches is the
228 presence of alternative but readily available outer membrane components that could function as ligands for

host receptors. In addition, preceding research on endothelial cells, originally considered the main host target of rickettsiae, resulted in the identification of four probable host cell receptors [Ku70 (6), α2β1 (7), FGFR (8), Epac (9)]. However, selective targeting of those receptors, showed only moderate inhibition of *Rickettsia* invasion, indicating cooperative and/or alternative receptor-ligand systems for bacteria engulfment. Intriguingly, no receptor-ligand mechanism for rickettsial invasion has been identified for professional phagocytes, like MΦ. To address this knowledge gap, we focused on receptor-ligand systems involved in efferocytosis, a highly anti-inflammatory mechanism required for cellular homeostasis, which is often hijacked by pathogens, including viruses and bacteria, to promote their own host invasion (10–13, 25, 28). As this process involves the recognition of "eat me" signals [e.g., phosphatidylserine (PS)] on apoptotic cells (ACs) through various PS-receptors, including MerTK, TIM1/4, or CD300s (e.g., CD300f) (10–13, 25, 28), we took advantage of the well-established *CD300f* knockout mouse model (17). Our studies demonstrate that CD300f$^{-/-}$ but not WT mice were protected against *R. typhi*- or *R. rickettsii* [*Shelia Smith*]-induced fatal rickettsiosis. As preceding findings from other and our laboratory suggest that rickettsiae exhibit species-specific immune modulatory responses in MΦ to establish an intracellular niche (20, 21, 23, 29–36), we next evaluated the role of CD300f on MΦ during rickettsial infection. Using *in vivo* depletion and adoptative transfer studies we showed that CD300f-expressing MΦ are crucial in controlling rickettsial infection *in vivo*. Of note, our study did not evaluate a potential contributing role of other CD300f-expressing cell types, including among other neutrophils or dendritic cells. CD300f has been shown to suppress the antimicrobial activity of neutrophils against *Pseudomonas aeruginosa* and *Candida albicans* infection (37). However, infection studies using pathogenic rickettsiae suggest that neutrophils do not alter the course of rickettsiosis or contribute to the restriction of bacterial growth (35). Dendritic cells seem to mount different immune responses against *R. conorii* infection dependent on the *in vivo* model (protective type 1 response in C57BL/6 mice vs. suppressive adaptive immunity in C3H/HeN animals) (38) Intriguingly, reports from other laboratory imply that in contrast to CD300f function on MΦ, its expression inhibited efferocytosis by dendritic cells (39) suggesting that CD300f might modulates rickettsiae infection and immune responses differently in dendritic cells as compared to MΦ, however the precise mechanism remains to be investigated.

As the CD300 family is composed of several members we next addressed the contributing rules of other family members using bone marrow-derived macrophages (BMDMΦ) deficient in the expression of specific

257 CD300 receptors (e.g., CD300d), and showed that CD300f, but not CD300d, plays a predominant rule in
258 facilitating pathogenic rickettsiae infection. However, it is well-known that MΦ express additional PS-binding
259 receptors, including among others Ku70 (40), CD300b (18, 22), Tim4 (41), and BAI1 (42), so it is plausible that
260 CD300f can directly or indirectly cooperate with other receptors to modulate phagocytosis of their cargo, a
261 mechanism described for Tim4 (43) and future experiments will address these questions.

262 As CD300f-receptor engagement by rickettsiae would likely involve a ligand, we searched for putative
263 ligands on the rickettsial outer membrane and found the presence of several glycerophospholipids (GPLs) (44,
264 45), including among others phosphatidylserine (PS), and phosphatidylglycerol (PG), known "eat-me" signals
265 involved in efferocytosis (10–12, 28). Preceding findings by others and our work described that obligate
266 intracellular bacteria, like *Rickettsia* spp possess most enzymes required for biosynthesis of
267 glycerophospholipids, like PS, however with some metabolic holes, because of missing enzymes in the
268 biosynthetic pathway, illustrating the dependence on host precursor to synthesize downstream metabolites
269 (46–48). Based on these findings we hypothesized that *Rickettsia* engulfment is mediated by a CD300f-PS
270 systems generally used for efferocytosis. We assessed the importance of bacterial PS for engulfment in WT
271 BMDMΦ by pre-incubating *R. typhi* and *R. rickettsii* with increasing concentrations of recombinant Annexin V
272 (rAnxV), a molecule known to block PS-mediated efferocytosis (16, 17), prior to infection and showed that
273 rAnxV reduced the engulfment of *R. typhi* or *R. rickettsii* in a dose-dependent manner. However, it is important
274 to note that not all externalized PS functions equivalent, and therefore it is feasible that the PS found on the
275 bacterial outer membrane is not involved in the phagocytosis process directly, which was described for other
276 cells [(e.g., monocytes and macrophages (49, 50)]. It is also plausible that the PS promoting *Rickettsia*
277 engulfment is provided by a bystander AC remnant, a mechanism described for *Trypanosoma brucei* (51), or
278 via a PS-cloaking mechanism a pathway described for *Listeria monocytogenes* (52). Thus, our findings
279 suggest that PS modulates the pathogenic rickettsiae engulfment into BMDMΦ via CD300f, however the
280 source of PS and therefore the precise mechanism of CD300f-dependent phagocytosis of rickettsiae requires
281 further investigation.

282 Findings from others and our laboratory further suggests that IL-1 signaling responses played a critical role
283 in limiting rickettsial infection *in vivo* and *in vitro* (20, 21, 29, 33–35, 53). Specifically, we showed that both *R.*
284 *typhi* and *R. rickettsii* reduced IL-1α and IL-1β (to a lesser extent) responses, in order, to establish an

285 intracytosolic replication niche in MΦ. As the CD300f-PS-mediated signaling response is a highly immune-
286 suppressive event, we evaluated the pro- and anti-inflammatory cytokine responses in WT and CD300f$^{-/-}$
287 BMDMΦ during *R. typhi* and *R. rickettsii* infection. Our data suggest that the survival advantage of *R. typhi* and
288 *R. rickettsii* within WT BMDMΦ is due to a CD300f-mediated increase in the expression of anti-inflammatory
289 IL-10 levels, and a decrease in anti-rickettsial IL-1α and IL-1β cytokine responses. In line with our findings,
290 previous reports suggest that CD300f augments fungal and bacterial infection by suppressing MyD88/TRIF-
291 mediated cytokine responses (37, 54–56). Given these reports by others and our recent findings, it is tempting
292 to speculate that pathogenic *Rickettsia* engage the CD300f receptor, likely via the PS ligand, to modulate anti-
293 inflammatory IL-10 levels and to suppress TLR- and inflammasome-mediated pro-inflammatory IL-1β and IL-1α
294 cytokine responses to establish an intracytosolic replication niche, however, the precise mechanism remains
295 unclear and requires further investigation.
296

297 **Materials and Methods**

298 **Animals**

299 All experiments were conducted in fully AAALAC-accredited program using 8- to 10-week-old female C57BL/6J
300 wild-type (WT), CD300d$^{-/-}$, or CD300f$^{-/-}$ mice in a specific-pathogen-free environment according to the
301 University of Maryland School of Medicine Institutional Animal Care and Use Committee (IACUC).
302

303 **Antibodies and Reagents**

304 Antibodies against whole *Rickettsia* (SFG or TG) were raised in house (20, 21, 23). ProLong Gold antifade
305 mounting medium with DAPI (4′,6-diamidino-2-phenylindole), paraformaldehyde (PFA), and Alexa 488/594-
306 conjugated secondary antibodies were purchased from Thermo Fisher Scientific.
307

308 **Bacterial strains, cell culture, and infection**

309 Vero76 cells (African green monkey kidney, ATCC, RL-1587) were maintained in minimal Dulbecco's modified
310 Eagle's medium (DMEM) supplemented with 10% heat-inactivated fetal bovine serum (FBS) at 37°C with 5%
311 CO_2. *R. rickettsii* (*Sheila Smith*) strain was obtained from Dr. Ted Hackstadt (Rocky Mountain Laboratories,
312 NIH, MT, USA) and *R. typhi* strain (Wilmington) was obtained from CDC. *Rickettsia* strains were propagated in

313 Vero76 cells grown in DMEM supplemented with 5% FBS at 34°C with 5% CO_2. All *Rickettsia* were partially
314 purified as described previously (57, 58). Partially purified *R. rickettsii* and *R. typhi* were used for infection of
315 BMDMΦ at 34°C. Taking into consideration of rickettsial doubling time of 8 to 10 h, we used higher MOI for
316 early stages of infection (~20 for 2 hours post infection (hpi) timepoint vs. MOI of 5 at later time points (24 and
317 48 h post-infection) (20, 23, 58–60). Tail vein injection (*i.v.*) of purified *Rickettsia* (10^5-10^6 PFU), resuspended
318 in PBS was used to initiate infection in mice as described previously as (20). At Days 1, 3, and 7 after
319 administration, blood was collected, and serum cytokine levels were measured by flow cytometry. Splenic
320 tissue specimens were collected at the indicated times and used for bacterial burden analysis by qPCR
321 described below.
322
323 **Differentiation of bone marrow-derived macrophages**
324 Bone marrow cells were isolated from femurs and tibias of WT, CD300d$^{-/-}$ or CD300f$^{-/-}$ mice. Differentiation was
325 induced by culturing bone marrow cells in RPMI 1640 medium supplemented with 10% FBS and 30% L929-
326 conditioned medium (a source of macrophage colony stimulating factor) and cultured for 7 days as described
327 previously (18, 20, 21).
328
329 **RNA isolation and quantitative real-time PCR**
330 To determine viable bacterial number during the course of host infection, we performed RT-qPCR assay on
331 isolated RNA (59, 61, 62). BMDMΦ samples were collected at different times of post infection, while spleens
332 were collected at day 7 post infection. RNA was extracted from 1 x 10^6 BMDMs or 100 µL of organ
333 homogenate using the Quick-RNA miniprep kit (ZymoResearch). The iScript Reverse Transcription Supermix
334 kit (Bio-Rad) was used to synthesize cDNAs from 200 ng of RNA according to the manufacturer's instructions.
335 Quantitative real-time PCR was performed using SYBR Green (Thermo Fisher Scientific), 2 µl cDNA and 1 µM
336 each of the following oligonucleotides for rickettsial (housekeeping) citrate synthase gene (*GltA*), and host
337 (housekeeping) *GAPDH* gene. Relative copy number (RCN) of *GltA* expression was normalized by the
338 expression of the *GAPDH* and calculated with the equation: RCN = $E^{-\Delta Ct}$, where E = efficiency of PCR, and Ct
339 = Ct *target* − Ct *GAPDH*. Melting curve analyses were performed at the end of each run to ensure that only
340 one product was amplified as described previously (20, 21, 63).

341

342 ***In vivo* depletion of macrophages following *Rickettsia* challenge**

343 C57/B6J WT or CD300f$^{-/-}$ mice were injected via tail vein (*i.v.*) using liposome-encapsulated PBS- or
344 dichloromethylene biphosphate (Cl_2MBP), as described previously (18, 20). Mice were injected twice (48 and
345 24 hrs) with PBS- or Cl_2MBP-liposomes (200 µl/per mouse) followed by injections (*i.v.*) twenty-four hours later
346 with 10^6 PFU of *R. typhi* or *R. rickettsii*. Survival was monitored for 7 days. Bacterial burden was determined in
347 spleens of uninfected or *R. typhi*- and *R. rickettsii*-injected mice by qPCR at day 7 (n = 5 for each treatment).

348

349 **Adoptive transfer of bone marrow derived macrophages following *Rickettsia* challenge**

350 C57/B6J WT mice were injected via tail vein (*i.v.*) Mice were injected twice (72 and 48 hrs) with PBS- or
351 Cl_2MBP-liposomes (200 µl/per mouse) followed by injections with BMDMΦ (5 x 10^6 cells/mouse) from CD300f$^{-/-}$
352 , or WT mice, as described previously (18, 20). Twenty-four hours later, mice were injected (*i.v.*) with 10^5 PFU
353 of *R. typhi* or *R. rickettsii*. Survival was monitored for 7 days, and bacterial burden was determined in spleens
354 of uninfected or *Rickettsia*-injected mice by qPCR.

355

356 **Immunofluorescence**

357 Eight-well chamber slides were seeded with WT, CD300d$^{-/-}$ or CD300f$^{-/-}$ BMDMΦ (30-50 x 10^4 cells/well) and
358 infected with partially purified pathogenic *Rickettsia* spp [MOI = 20 (2 h) and MOI = 5 (24 h)] as described
359 previously (20, 21, 23, 58–60). Briefly, BMDMΦ were incubated with partially purified *Rickettsia* for various
360 length of time at 34°C. Following incubation, cells were washed three times with 1 x PBS and fixed with 4%
361 paraformaldehyde (PFA) for 20 min at room temperature. Cells were than permeabilized in blocking buffer
362 (0.3% saponin and 0.5% normal goat serum in 1 x PBS) for 30 min and incubated for 1 h with antibodies
363 against whole *Rickettsia* (SFG or TG) using a dilution of 1:100 or 1:500 respectively. Cells were then washed
364 with 1 x PBS and incubated for 1 h with αAlexa Fluor 488 secondary antibody (1:1,500). Next, cells were
365 washed with 1 x PBS and mounted with ProLong Gold antifade mounting medium containing DAPI. Images
366 were acquired using the Nikon W-1 spinning disk confocal microscope (University of Maryland Baltimore,
367 Confocal Core Facility) and internalization was analyzed using Fiji software as described previously (23).
368 Approximately 100 host cells were enumerated for each experiment and each experiment was repeated five
369 times.

370 For infection assays using recombinant Annexin V protein, partially purified *Rickettsia* were incubated
371 with various concentrations of regular or heat inactivated recombinant Annexin V (rAnxV) for 0.5 h at 4°C and
372 reactions were used to infect BMDMΦ for additional 2 or 24 h at 34°C. Following incubation, cells were
373 washed, fixed, and stained with anti-*Rickettsia* antibodies as described above.
374

375 **Neutralization of IL-1α and IL-1β *in vitro***

376 For *in vitro* neutralization of IL-1α and IL-1β, *R. typhi*-, or *R. rickettsii*-infected BMDMΦ from C57BL/6J WT or
377 CD300f$^{-/-}$ mice were treated with 100 nM anti-IL-1α (clone ALF-161; BioXCell), anti-IL-1β (clone B122;
378 BioXCell), or IgG isotype control (Armenian hamster IgGs; BioXCell) antibodies for 24 h, and bacterial burden
379 was assessed by qPCR.
380

381 **Measurement of cytokines and chemokines**

382 Cytokine concentrations in supernatants from cultured BMDMΦ or sera of animals were assessed using the
383 Legendplex mouse inflammation kit (BioLegend) following the manufacturer's instructions as described
384 previously (18, 20).
385

386 **Statistical analysis**

387 Data sets were considered statistically significant when a $P \leq 0.05$ value was obtained by unpaired Student's *t*-
388 test (two-tailed), paired Student's *t*-test (two-tailed), a one-way ANOVA with either multiple comparisons or
389 comparison to WT bacteria, a two-way ANOVA, or a log-rank (Mantel-Cox) test. Statistical analyses were
390 performed using GraphPad Prism Software, version 8 and samples were denoted using the following asterisks:
391 *$P \leq 0.05$; **$P \leq 0.01$; ***$P \leq 0.005$; ****$P \leq 0.001$. Data are presented as mean ± SEM, unless stated otherwise.
392

393 **Acknowledgments**

394 We gratefully acknowledge Ted Hackstadt (Rocky Mountain Laboratories, NIH, MT, USA) for generously
395 providing us with essential biological specimens and reagents, including rickettsial strains. We would like to
396 thank Magda Beier-Sexton for her administrative, technical, organizational, and editorial contributions to the

397 manuscript. This work was supported with funds from the NIAID/NIH grants (R01AI017828 and R01AI126853
398 and R21AI166821).
399

400 **Conflicts of Interest**

401 The authors declare no conflict of interest. The funding sources had no role in the design of the study, in the
402 collection, analyses, or interpretation of data, in the writing of the manuscript, or in the decision to publish the
403 results.
404

405 **Figure legends**

406 **Fig.1. Efferocytic receptor, CD300f, exacerbates the pathogenesis of rickettsiosis.** C57BL/6J WT or
407 CD300f$^{-/-}$ mice were injected via tail vein (*i.v.*) with *R. typhi* (A-B), *R. rickettsii* (C-D), or PBS (10^6 PFU, n = 12
408 for each treatment). Survival was monitored for 7 days. (B and D) Bacterial burden was tested in spleens of *R.*
409 *typhi*-, *R. rickettsii*-, or PBS-injected WT and CD300f$^{-/-}$ mice (n = 5 per each treatment) shown in panels B to D
410 by *GltA* reverse transcription quantitative real-time PCR (RT-qPCR) at day 3 and 7 (n = 5 for each treatment).
411 Relative copy number (RCN) of *GltA* expression of rickettsiae was normalized by the expression of the
412 housekeeping host gene, *GAPDH*. Error bars in panels B to D represent means ± SEM from five independent
413 experiments. NS, nonsignificant; $^{**}P \leq 0.01$; $^{***}P \leq 0.005$.
414

415 **Fig. 2. Macrophages are critical in restricting pathogenic rickettsiae infection *in vivo*.** (A) C57/B6J WT or
416 CD300f$^{-/-}$-deficient mice (n = 12 per experimental group) were *i.v.* injected twice (48 and 24 hrs) with PBS- or
417 Cl_2MBP-liposomes (200 μl/per mouse) followed by *i.v.* injections with 10^5 PFU of either *R. typhi* (B-C) or *R.*
418 *rickettsii* (D-E). Survival was monitored for 7 days. Bacterial burden (C and E) was determined in spleens of
419 *Rickettsia*-injected WT or CD300f$^{-/-}$ mice as described in the legend of Fig.1. Error bars in (C, and E) represent
420 means ± SEM; NS, non-significant; $^{*}P \leq 0.05$; $^{**}P \leq 0.01$; $^{***}P \leq 0.005$.
421

422 **Fig. 3. CD300f on macrophages facilitates pathogenic rickettsiae infection *in vivo*.** C57/B6J WT mice (n
423 = 12 per experimental group) were injected via tail vein (*i.v.*) using liposome-encapsulated PBS- or
424 dichloromethylene biphosphate (Cl_2MBP). Mice were injected twice (72 and 48 hrs) with PBS- or Cl2MBP-

425 liposomes (200 µl/per mouse) followed by injections with BMDMΦ (5 x 10^6 cells/mouse) from CD300f$^{-/-}$, or WT
426 mice. Twenty-four hours later, mice were injected (*i.v.*) with 10^5 PFU of *R. typhi* (B-C) or *R. rickettsii* (D-E).
427 Survival was monitored for 7 days. Bacterial burden (C, E) was determined in spleens of *R. typhi*- and *R.*
428 *rickettsii*-injected WT mice as described in the legend of Fig.1. Error bars in (C, E) represent means ± SEM;
429 NS, non-significant; *$P \leq 0.05$; **$P \leq 0.01$; ***$P \leq 0.005$.
430
431 **Fig. 4. CD300f facilitates *Rickettsia* invasion by reducing pro-inflammatory IL-1 cytokine responses.**
432 BMDMΦ from WT, CD300f$^{-/-}$ and CD300d$^{-/-}$ mice were infected with *R. typhi* or *R. rickettsii* at a multiplicity of
433 infection (MOI) of 20 (2 h) and 5 (24 h). (A) Number of *Rickettsia* per cell was determined 2 h post-infection by
434 immunofluorescent assay (IFA) using anti-Alexa488 or anti-Alexa595 conjugated anti-*R. typhi* or anti-*R.*
435 *rickettsii* antibody staining's. Experimental data were repeated 5 times and represent approximately 100–200
436 bacteria for each experimental group and time point. (B) Bacterial burden in *R. typhi*- and *R. rickettsii*-infected
437 BMDMΦ was determined 24 h (n = 5 per group) post-infection by *GltA* RT-qPCR. RCN of *GltA* expression was
438 normalized by the expression of *GAPDH*. (C) Culture supernatants from BMDMΦ from WT, CD300f$^{-/-}$ and
439 CD300d$^{-/-}$ mice infected with *R. typhi* or *R. rickettsii* were analyzed for production of IL-1α, IL-1β, and IL-10
440 using Legendplex kits (BioLegend), followed by flow cytometry. (D-E) Bacterial burdens in *Rickettsia*-infected
441 WT, CD300f$^{-/-}$ and CD300d$^{-/-}$ treated BMDMΦ with anti-IL-1α, anti-IL-1β, both anti-IL-1α and anti-IL-1β
442 antibodies, or corresponding IgG isotype controls. Samples were evaluated at 24 h post-infection by *GltA* RT-
443 qPCR and normalized by *GAPDH* levels. Error bars in (A-D) represent means ± SEM; NS, non-significant; *$P \leq$
444 0.05; **$P \leq 0.01$; ***$P \leq 0.005$; ****$P \leq 0.001$.
445
446 **Supplemental figure legends**
447 **Fig. S1. Splenic data during infection of pathogenic *Rickettsia* species.** (A) Representative images of
448 spleens (at Day 7) from C57BL/6J WT and CD300f$^{-/-}$ mice injected *i.v.* with *R. typhi*, *R. rickettsii*, or PBS (dose
449 of 10^6 PFU). (B) Spleen weight from injected animals was evaluated at day 7 day (n = 8). Error bars in panel B
450 represent means ± SEM from five independent experiments. NS, nonsignificant; ****$P \leq 0.001$.
451

452 **Fig. S2. Splenic data after PBS- or Cl_2MBP-liposome treatment and rickettsiae infection.** (A-B) C57/B6J
453 WT or CD300f$^{-/-}$-deficient mice were *i.v.* injected twice (48 and 24 h) with PBS- or Cl_2MBP-liposomes (200
454 μl/per mouse) followed by *i.v.* injections with 10^5 PFU of either *R. typhi* (A) or *R. rickettsii* (B). Spleen weight
455 from injected animals was evaluated at day 7 day (n = 8). Error bars in panels A and B represent means ± SEM
456 from five independent experiments. NS, nonsignificant; ***P* ≤ 0.01; ****P* ≤ 0.005.
457
458 **Fig. S3. Splenic data after adaptive transfer of WT or CD300f$^{-/-}$-BMDM into WT mice during rickettsiae**
459 **infection.** (A-B) C57/B6J WT or CD300f$^{-/-}$-deficient mice were *i.v.* injected twice (48 and 24 h) with PBS- or
460 Cl_2MBP-liposomes (200 μl/per mouse) followed by injections with BMDMΦ (5 x 10^6 cells/mouse) from CD300f$^{-/-}$
461 , or WT mice. Twenty-four hours later, mice were injected (*i.v.*) with 10^5 PFU with 10^5 PFU of either *R. typhi* (A)
462 or *R. rickettsii* (B). Spleen weight from injected animals was evaluated at day 7 day (n = 8). Error bars in panels
463 A and B represent means ± SEM from five independent experiments. NS, nonsignificant; ***P* ≤ 0.01; ****P* ≤
464 0.005.
465
466 **Fig. S4. Blocking phosphatidylserine reduced the invasion of pathogenic rickettsiae into macrophages.**
467 (A-B) Purified *R. typhi* or *R. rickettsii* were pretreated for 0.5 h with various amounts of recombinant Annexin
468 (rAxnV) and then utilized to infect BMDMΦ from WT mice. BMDMΦ were infected with *R. typhi* or *R. rickettsii*
469 (untreated or pretreated with rAxnV) at a multiplicity of infection (MOI) of 20 (2 h) and 5 (24 h). Boiled rAnxV
470 served as control. (A) Number of *Rickettsia* per cell was determined by immunofluorescent assay (IFA) using
471 anti-Alexa488 or anti-Alexa595 conjugated anti-*R. typhi* or anti-*R. rickettsii* antibody staining's. Experimental
472 data were repeated 5 times and represent approximately 100 - 200 bacteria for each experimental group and
473 time point. (B) Bacterial burden in *R. typhi*- and *R. rickettsii*-infected BMDMΦ, as described in panel (A), was
474 determined 24 h (n = 5 per group) post-infection by *GltA* RT-qPCR. RCN of *GltA* expression was normalized
475 by the expression of *GAPDH*. Error bars in panels A and B represent means ± SEM from five independent
476 experiments. NS, nonsignificant; **P* ≤ 0.05; ***P* ≤ 0.01; ****P* ≤ 0.005.
477
478 **Fig. S5 Assessment of IL-1α and IL-1β cytokine responses in Rickettsia-infected WT and CD300f$^{-/-}$**
479 **macrophages treated with IL-1α, IL-1β, or IgG-isotype control antibodies.** (A-B) Culture supernatants of

480 uninfected, *R. typhi*-, or *R. rickettsii*-infected WT and CD300f$^{-/-}$ BMDMΦ treated with anti-IL-1α, anti-IL-1β, both
481 anti-IL-1α/anti-IL-1β antibodies, or IgG-isotype controls. Samples were evaluated 24 h post-infection to
482 determine the level of IL-1β and IL-1α cytokines using Legendplex kits (BioLegend) followed by flow cytometry.
483 Error bars (A-B) represent means ± SEM from five independent experiments; NS: non-significant; **P*≤ 0.05; ***P*
484 ≤ 0.01; ****P* ≤ 0.005.

485

486 **Reference**:

487 1. N. A. Drexler, *et al.*, Fatal Rocky Mountain Spotted Fever along the United States-Mexico Border, 2013-
488 2016. *Emerg Infect Dis* **23**, 1621–1626 (2017).
489 2. S. A. Billeter, M. E. Metzger, Limited Evidence for Rickettsia felis as a Cause of Zoonotic Flea-Borne
490 Rickettsiosis in Southern California. *J Med Entomol* **54**, 4–7 (2017).
491 3. L. S. Blanton, *et al.*, Opossums and cat fleas: New insights in the ecology of murine typhus in
492 Galveston, Texas. *American Journal of Tropical Medicine and Hygiene* **95**, 457–461 (2016).
493 4. A. Sahni, R. Fang, S. K. Sahni, D. H. Walker, Pathogenesis of Rickettsial Diseases: Pathogenic and
494 Immune Mechanisms of an Endotheliotropic Infection. *Annu Rev Pathol* **14**, 127–152 (2019).
495 5. O. H. Voss, M. S. Rahman, Rickettsia-host interaction: strategies of intracytosolic host colonization.
496 *Pathog Dis* **79** (2021).
497 6. J. J. Martinez, S. Seveau, E. Veiga, S. Matsuyama, P. Cossart, Ku70, a component of DNA-dependent
498 protein kinase, is a mammalian receptor for Rickettsia conorii. *Cell* **123**, 1013–1023 (2005).
499 7. R. D. Hillman, Y. M. Baktash, J. J. Martinez, OmpA-mediated rickettsial adherence to and invasion of
500 human endothelial cells is dependent upon interaction with α2β1 integrin. *Cell Microbiol* **15**, 727–741
501 (2013).
502 8. A. Sahni, *et al.*, Fibroblast growth factor receptor-1 mediates internalization of pathogenic spotted fever
503 rickettsiae into host endothelium. *PLoS One* **12** (2017).
504 9. B. Gong, *et al.*, Exchange protein directly activated by cAMP plays a critical role in bacterial invasion
505 during fatal rickettsioses. *Proceedings of the National Academy of Sciences* **110**, 19615–19620 (2013).
506 10. R. S. Flannagan, V. Jaumouillé, S. Grinstein, The Cell Biology of Phagocytosis. *Annual Review of*
507 *Pathology: Mechanisms of Disease* **7**, 61–98 (2012).
508 11. O. H. Voss, L. Tian, Y. Murakami, J. E. Coligan, K. Krzewski, Emerging role of CD300 receptors in
509 regulating myeloid cell efferocytosis. *Mol Cell Oncol* (2015).
510 https://doi.org/10.4161/23723548.2014.964625.
511 12. R. B. Birge, *et al.*, Phosphatidylserine is a global immunosuppressive signal in efferocytosis, infectious
512 disease, and cancer. *Cell Death Differ* **23**, 962–978 (2016).
513 13. J. Vitallé, I. Terrén, A. Orrantia, O. Zenarruzabeitia, F. Borrego, CD300 receptor family in viral infections.
514 *Eur J Immunol* **49**, 364–374 (2019).
515 14. G. J. Clark, X. Ju, C. Tate, D. N. J. Hart, The CD300 family of molecules are evolutionarily significant
516 regulators of leukocyte functions. *Trends Immunol* **30**, 209–217 (2009).
517 15. F. Borrego, The CD300 molecules: An emerging family of regulators of the immune system. *Blood*
518 (2013). https://doi.org/10.1182/blood-2012-09-435057.
519 16. S.-C. Choi, *et al.*, Cutting Edge: Mouse CD300f (CMRF-35–Like Molecule-1) Recognizes Outer
520 Membrane-Exposed Phosphatidylserine and Can Promote Phagocytosis. *The Journal of Immunology*
521 (2011). https://doi.org/10.4049/jimmunol.1101549.
522 17. L. Tian, *et al.*, P85α recruitment by the CD300f phosphatidylserine receptor mediates apoptotic cell
523 clearance required for autoimmunity suppression. *Nat Commun* (2014).
524 https://doi.org/10.1038/ncomms4146.
525 18. O. H. Voss, *et al.*, Lipopolysaccharide-Induced CD300b Receptor Binding to Toll-like Receptor 4 Alters
526 Signaling to Drive Cytokine Responses that Enhance Septic Shock. *Immunity* **44**, 1365–1378 (2016).
527 19. H. N. Lee, *et al.*, Dendritic cells expressing immunoreceptor CD300f are critical for controlling chronic
528 gut inflammation. *Journal of Clinical Investigation* (2017). https://doi.org/10.1172/JCI89531.

20. O. H. Voss, *et al.*, Pathogenic, but Not Nonpathogenic, Rickettsia spp. Evade Inflammasome-Dependent IL-1 Responses To Establish an Intracytosolic Replication Niche. *mBio* **13** (2022).
21. O. H. Voss, *et al.*, Autophagy facilitates intracellular survival of pathogenic rickettsiae in macrophages via evasion of autophagosomal maturation and reduction of microbicidal pro-inflammatory IL-1 cytokine responses. *Microbiol Spectr* **11**, e0279123 (2023).
22. Y. Murakami, *et al.*, CD300b regulates the phagocytosis of apoptotic cells via phosphatidylserine recognition. *Cell Death Differ* (2014). https://doi.org/10.1038/cdd.2014.86.
23. O. H. Voss, *et al.*, Risk1, a Phosphatidylinositol 3-Kinase Effector, Promotes Rickettsia typhi Intracellular Survival. *mBio* **11** (2020).
24. N. Personnic, K. Bärlocher, I. Finsel, H. Hilbi, Subversion of Retrograde Trafficking by Translocated Pathogen Effectors. *Trends Microbiol* **24**, 450–462 (2016).
25. K. Ray, B. Marteyn, P. J. Sansonetti, C. M. Tang, Life on the inside: the intracellular lifestyle of cytosolic bacteria. *Nat Rev Microbiol* **7**, 333–340 (2009).
26. N. F. Noriea, T. R. Clark, T. Hackstadt, Targeted Knockout of the Rickettsia rickettsii OmpA Surface Antigen Does Not Diminish Virulence in a Mammalian Model System. *mBio* **6**, 1–9 (2015).
27. H.-M. M. Feng, T. Whitworth, J. P. Olano, V. L. Popov, D. H. Walker, Fc-dependent polyclonal antibodies and antibodies to outer membrane proteins A and B, but not to lipopolysaccharide, protect SCID mice against fatal Rickettsia conorii infection. *Infect. Immun* **72**, 2222–2228 (2004).
28. K. S. Ravichandran, Find-me and eat-me signals in apoptotic cell clearance: progress and conundrums. *J Exp Med* **207**, 1807–1817 (2010).
29. J. Bechelli, *et al.*, Atg5 supports Rickettsia australis infection in macrophages in vitro and in vivo. *Infect Immun* **87** (2019).
30. T. P. Burke, *et al.*, Inflammasome-mediated antagonism of type I interferon enhances Rickettsia pathogenesis. *Nat Microbiol* **5**, 688–696 (2020).
31. P. Engström, *et al.*, Evasion of autophagy mediated by Rickettsia surface protein OmpB is critical for virulence. *Nat Microbiol* **4**, 2538–2551 (2019).
32. G. M. Borgo, *et al.*, A patatin-like phospholipase mediates Rickettsia parkeri escape from host membranes. *Nat Commun* **13** (2022).
33. C. Rumfield, I. Hyseni, J. W. McBride, D. H. Walker, R. Fang, Activation of ASC inflammasome driven by toll-like receptor 4 contributes to host immunity against rickettsial infection. *Infect Immun* **88** (2020).
34. C. Smalley, *et al.*, Rickettsia australis Activates Inflammasome in Human and Murine Macrophages. *PLoS One* **11**, e0157231 (2016).
35. S. Papp, *et al.*, Liver Necrosis and Lethal Systemic Inflammation in a Murine Model of Rickettsia typhi Infection: Role of Neutrophils, Macrophages and NK Cells. *PLoS Negl Trop Dis* **10**, e0004935 (2016).
36. K. Moderzynski, *et al.*, CD4+T Cells Are as Protective as CD8+T Cells against Rickettsia typhi Infection by Activating Macrophage Bactericidal Activity. *PLoS Negl Trop Dis* **10** (2016).
37. K. Ueno, *et al.*, Mouse LIMR3/CD300f is a negative regulator of the antimicrobial activity of neutrophils. *Sci Rep* **8**, 17406 (2018).
38. R. Fang, *et al.*, Differential interaction of dendritic cells with Rickettsia conorii: impact on host susceptibility to murine spotted fever rickettsiosis. *Infect Immun* **75**, 3112–23 (2007).
39. L. Tian, *et al.*, Enhanced efferocytosis by dendritic cells underlies memory T-cell expansion and susceptibility to autoimmune disease in CD300f-deficient mice. *Cell Death Differ* **23**, 1086–96 (2016).
40. H. Sun, Q. Li, G. Yin, X. Ding, J. Xie, Ku70 and Ku80 participate in LPS-induced pro-inflammatory cytokines production in human macrophages and monocytes. *Aging* **12**, 20432–20444 (2020).
41. M. Miyanishi, *et al.*, Identification of Tim4 as a phosphatidylserine receptor. *Nature* (2007). https://doi.org/10.1038/nature06307.
42. D. Park, *et al.*, BAI1 is an engulfment receptor for apoptotic cells upstream of the ELMO/Dock180/Rac module. *Nature* **450**, 430–434 (2007).
43. C. Nishi, S. Toda, K. Segawa, S. Nagata, Tim4- and MerTK-Mediated Engulfment of Apoptotic Cells by Mouse Resident Peritoneal Macrophages. *Mol Cell Biol* **34**, 1512–1520 (2014).
44. H. H. Winkler, E. T. Miller, Phospholipid composition of Rickettsia prowazeki grown in chicken embryo yolk sacs. *J Bacteriol* (1978).
45. T. Tzianabos, C. W. Moss, J. E. McDade, Fatty acid composition of rickettsiae. *J Clin Microbiol* (1981).
46. M. Lin, *et al.*, Host membrane lipids are trafficked to membranes of intravacuolar bacterium Ehrlichia chaffeensis. *Proceedings of the National Academy of Sciences* **117**, 8032–8043 (2020).

47. A. V, B. CA, B. TP, N. DK, W. MD, A Metabolic Dependency for Host Isoprenoids in the Obligate Intracellular Pathogen Rickettsia parkeri Underlies a Sensitivity to the Statin Class of Host-Targeted Therapeutics. *mSphere* **4** (2019).
48. T. P. Driscoll, *et al.*, Wholly *Rickettsia* ! Reconstructed Metabolic Profile of the Quintessential Bacterial Parasite of Eukaryotic Cells. *mBio* **8**, e00859-17 (2017).
49. M. K. Callahan, P. Williamson, R. A. Schlegel, Surface expression of phosphatidylserine on macrophages is required for phagocytosis of apoptotic thymocytes. *Cell Death Differ* **7**, 645–653 (2000).
50. U. Appelt, *et al.*, Viable, apoptotic and necrotic monocytes expose phosphatidylserine: Cooperative binding of the ligand Annexin V to dying but not viable cells and implications for PS-dependent clearance [2]. *Cell Death Differ* [Preprint] (2005).
51. R. A. DaMatta, *et al.*, Trypanosoma cruzi exposes phosphatidylserine as an evasion mechanism. *FEMS Microbiol Lett* **266**, 29–33 (2007).
52. M. A. Czuczman, *et al.*, Listeria monocytogenes exploits efferocytosis to promote cell-to-cell spread. *Nature* **509**, 230–234 (2014).
53. J. Bechelli, *et al.*, Subversion of Host Innate Immunity by Rickettsia australis via a Modified Autophagic Response in Macrophages. *Front Immunol* **0**, 962 (2021).
54. A. Martínez-Barriocanal, E. Comas-Casellas, S. Schwartz, M. Martín, J. Sayós, CD300 heterocomplexes, a new and family-restricted mechanism for myeloid cell signaling regulation. *J Biol Chem* **285**, 41781–94 (2010).
55. E.-J. Kim, S.-M. Lee, K. Suk, W.-H. Lee, CD300a and CD300f differentially regulate the MyD88 and TRIF-mediated TLR signalling pathways through activation of SHP-1 and/or SHP-2 in human monocytic cell lines. *Immunology* **135**, 226–35 (2012).
56. S.-M. Lee, E.-J. Kim, K. Suk, W.-H. Lee, CD300F blocks both MyD88 and TRIF-mediated TLR signaling through activation of Src homology region 2 domain-containing phosphatase 1. *J Immunol* **186**, 6296–303 (2011).
57. S. J. Kaur, *et al.*, TolC-dependent secretion of an ankyrin repeat-containing protein of *Rickettsia typhi*. *J Bacteriol* **194**, 4920–32 (2012).
58. K. E. Rennoll-Bankert, *et al.*, Which Way In? The RalF Arf-GEF Orchestrates Rickettsia Host Cell Invasion. *PLoS Pathog* **11**, e1005115 (2015).
59. M. S. Rahman, N. C. Ammerman, K. T. Sears, S. M. Ceraul, A. F. Azad, Functional characterization of a phospholipase A(2) homolog from Rickettsia typhi. *J Bacteriol* **192**, 3294–3303 (2010).
60. K. E. Rennoll-Bankert, *et al.*, RalF-Mediated Activation of Arf6 Controls Rickettsia typhi Invasion by Co-Opting Phosphoinositol Metabolism. *Infect Immun* **84**, 3496–3506 (2016).
61. P. G. Klein, V. K. Juneja, Sensitive detection of viable Listeria monocytogenes by reverse transcription-PCR. *Appl Environ Microbiol* **63**, 4441–4448 (1997).
62. S. Yaron, K. R. Matthews, A reverse transcriptase-polymerase chain reaction assay for detection of viable Escherichia coli O157:H7: investigation of specific target genes. *J Appl Microbiol* **92**, 633–640 (2002).
63. S. A. Rennoll, *et al.*, The cat flea (Ctenocephalides felis) immune deficiency signaling pathway regulates Rickettsia typhi infection. *Infect Immun* **86** (2018).

Fig. 1

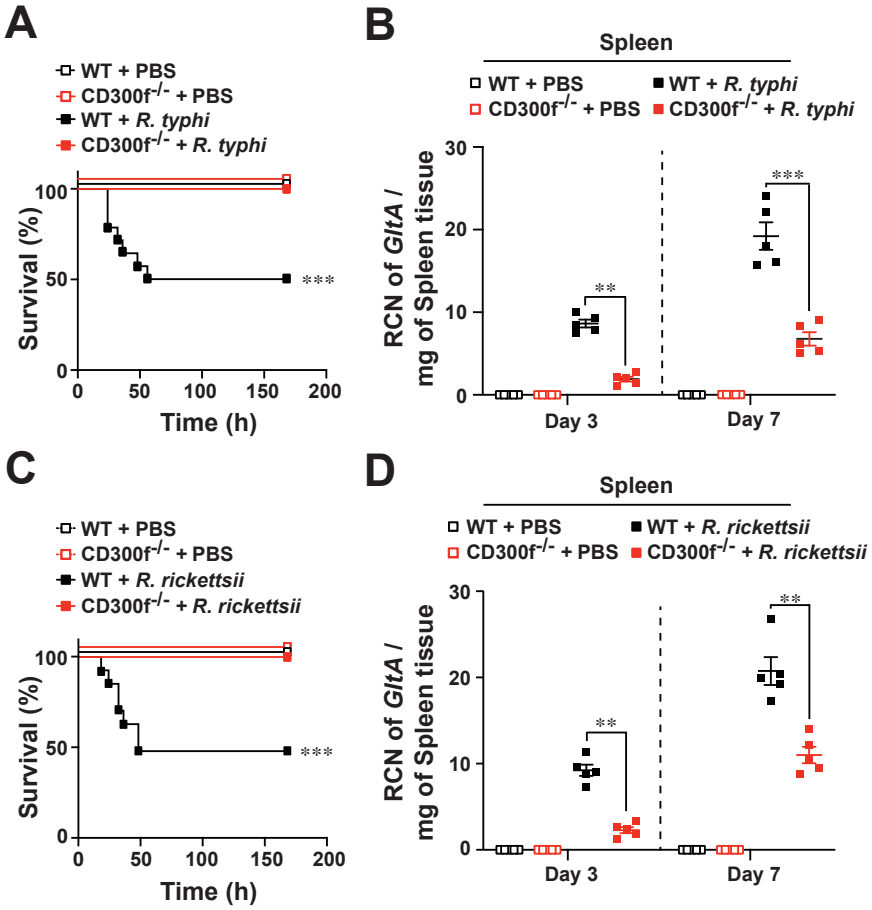
A
WT + PBS
CD300f-/- + PBS
WT + R. typhi
CD300f-/- + R. typhi
Survival (%)
Time (h)
***
B
Spleen
WT + PBS
WT + R. typhi
CD300f-/- + PBS
CD300f-/- + R. typhi
RCN of GltA / mg of Spleen tissue
Day 3
Day 7
**
***
C
WT + PBS
CD300f-/- + PBS
WT + R. rickettsii
CD300f-/- + R. rickettsii
Survival (%)
Time (h)
***
D
Spleen
WT + PBS
WT + R. rickettsii
CD300f-/- + PBS
CD300f-/- + R. rickettsii
RCN of GltA / mg of Spleen tissue
Day 3
Day 7
**
**

Fig. 2

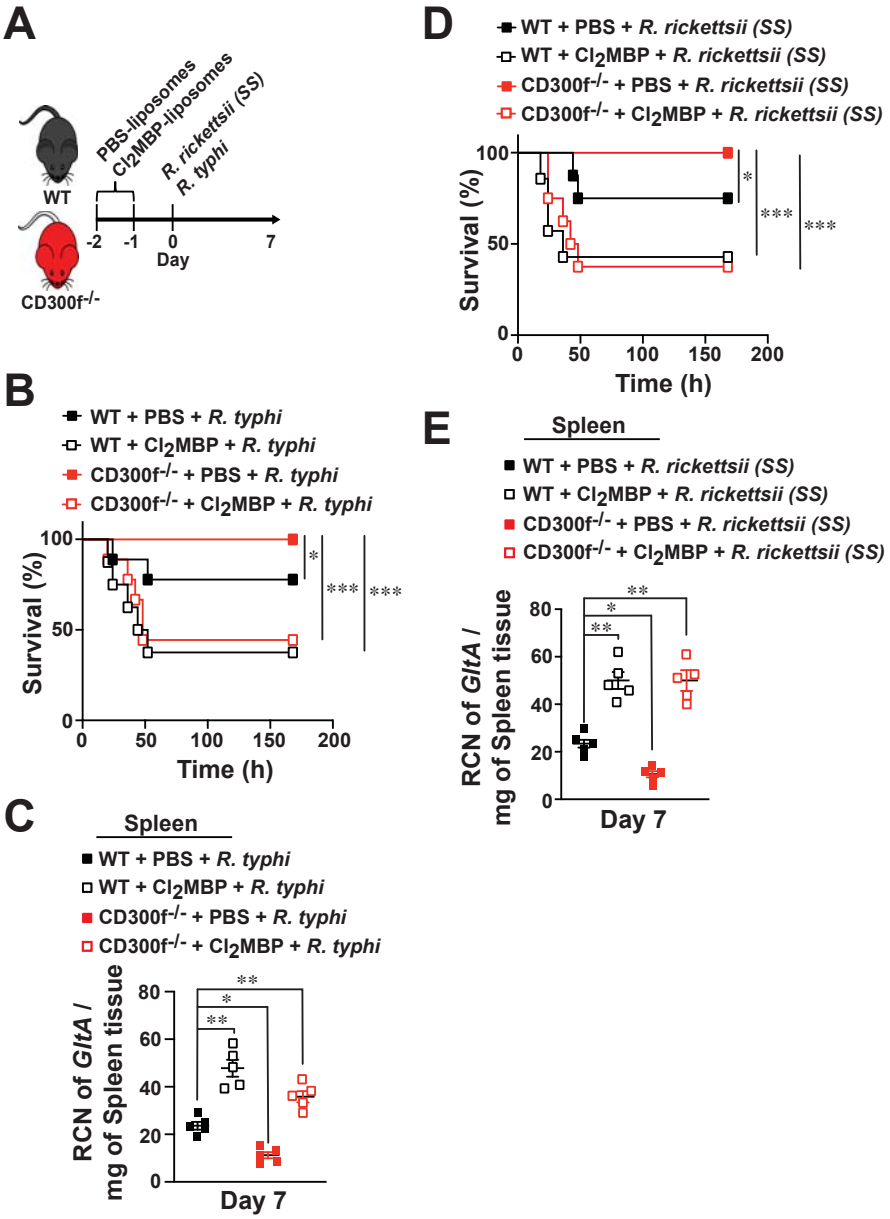
A
WT
CD300f-/-
PBS-liposomes
Cl2MBP-liposomes
R. rickettsii (SS)
R. typhi
-2
-1
0
7
Day
B
WT + PBS + R. typhi
WT + Cl2MBP + R. typhi
CD300f-/- + PBS + R. typhi
CD300f-/- + Cl2MBP + R. typhi
Survival (%)
Time (h)
C
Spleen
RCN of GltA / mg of Spleen tissue
Day 7
D
WT + PBS + R. rickettsii (SS)
WT + Cl2MBP + R. rickettsii (SS)
CD300f-/- + PBS + R. rickettsii (SS)
CD300f-/- + Cl2MBP + R. rickettsii (SS)
E

Fig. 3

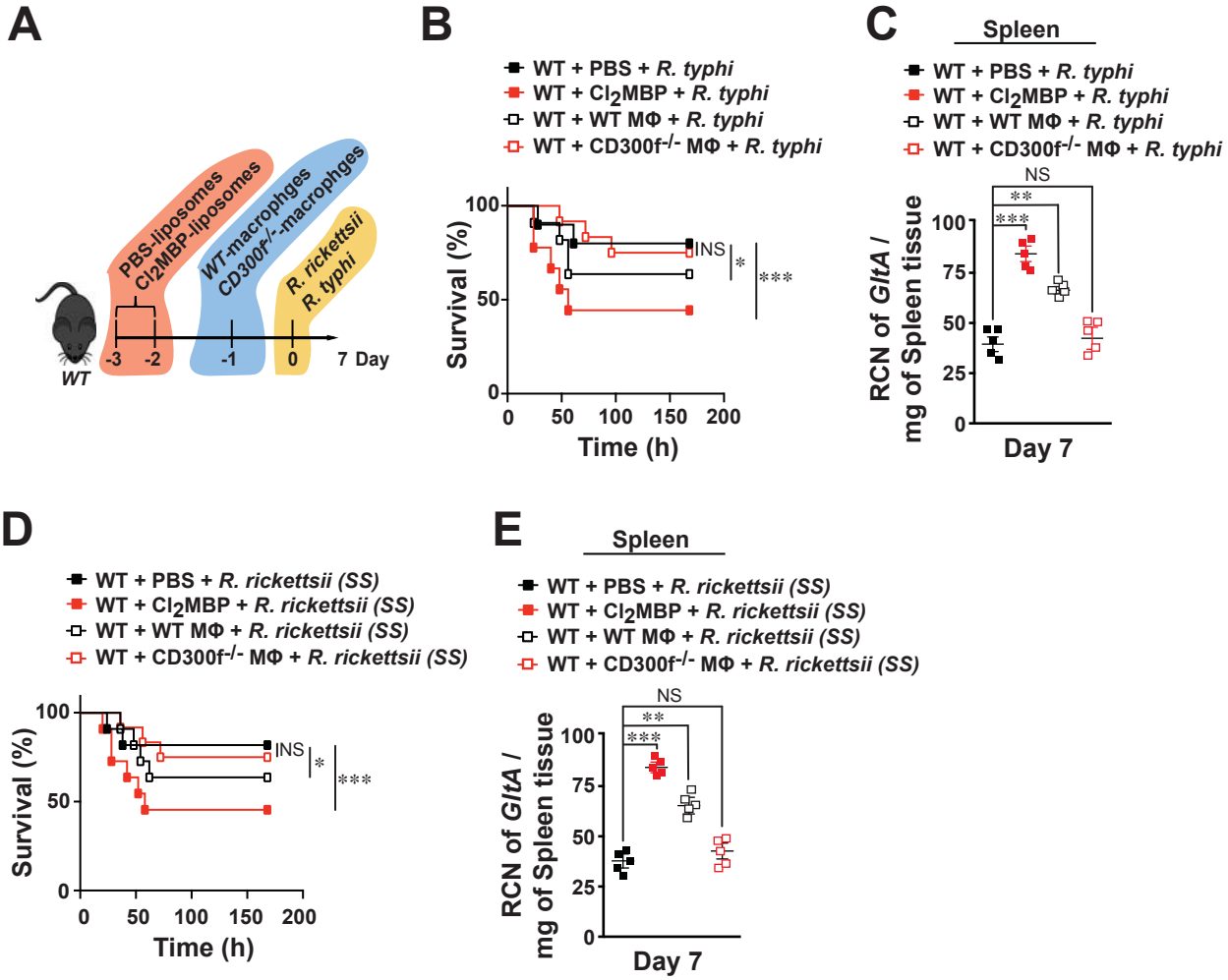
A
PBS-liposomes
Cl2MBP-liposomes
WT-macrophges
CD300f-/--macrophges
R. rickettsii
R. typhi
WT
-3
-2
-1
0
7 Day
B
WT + PBS + R. typhi
WT + Cl2MBP + R. typhi
WT + WT MΦ + R. typhi
WT + CD300f-/- MΦ + R. typhi
Survival (%)
Time (h)
INS
*
***
C
Spleen
WT + PBS + R. typhi
WT + Cl2MBP + R. typhi
WT + WT MΦ + R. typhi
WT + CD300f-/- MΦ + R. typhi
NS
**
***
RCN of GltA / mg of Spleen tissue
Day 7
D
WT + PBS + R. rickettsii (SS)
WT + Cl2MBP + R. rickettsii (SS)
WT + WT MΦ + R. rickettsii (SS)
WT + CD300f-/- MΦ + R. rickettsii (SS)
Survival (%)
Time (h)
INS
*
***
E
Spleen
WT + PBS + R. rickettsii (SS)
WT + Cl2MBP + R. rickettsii (SS)
WT + WT MΦ + R. rickettsii (SS)
WT + CD300f-/- MΦ + R. rickettsii (SS)
NS
**
***
RCN of GltA / mg of Spleen tissue
Day 7

Fig. 4

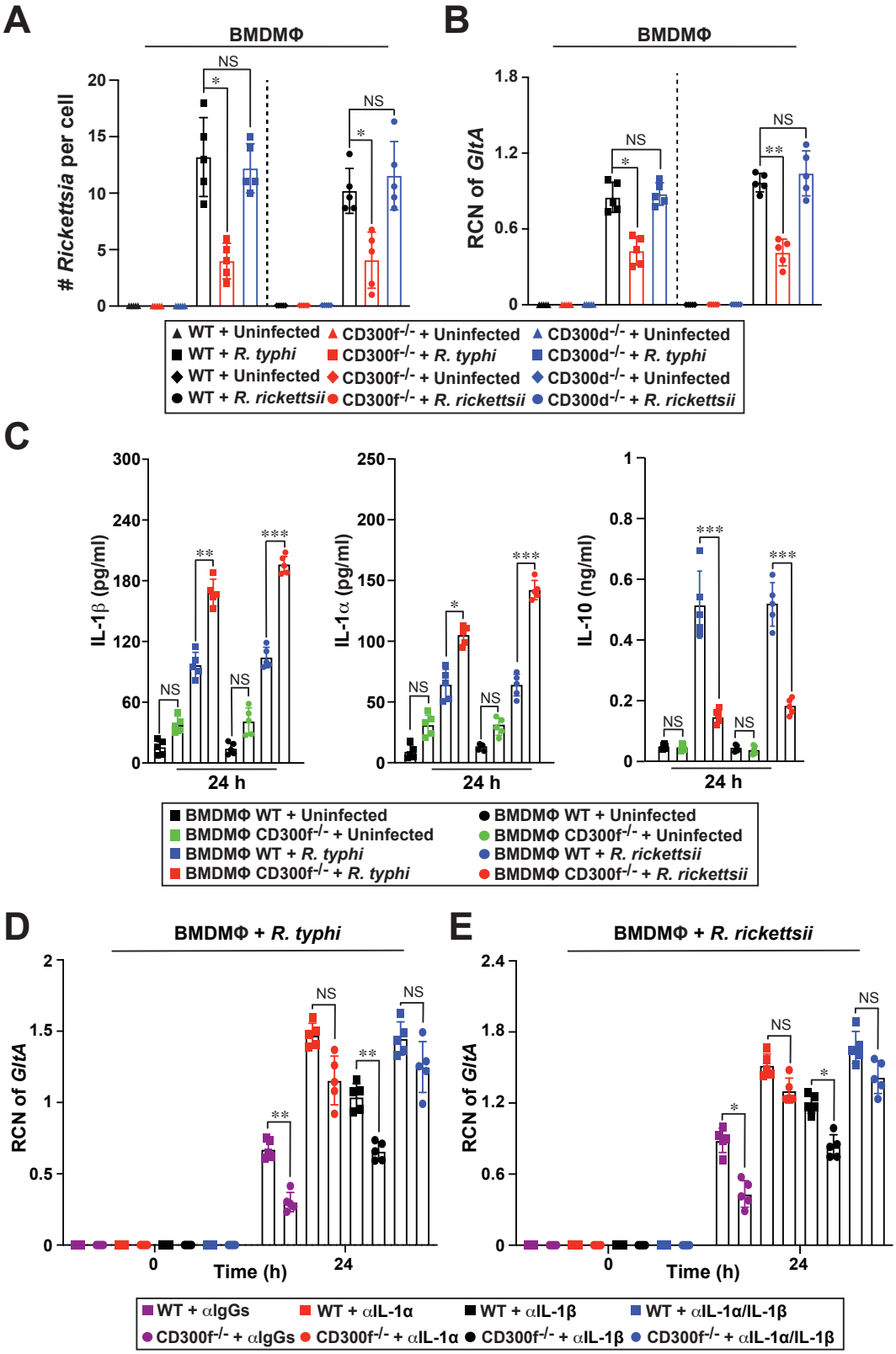
A
BMDMΦ
Rickettsia per cell
NS
*
B
BMDMΦ
RCN of GltA
**
WT + Uninfected
WT + R. typhi
WT + Uninfected
WT + R. rickettsii
CD300f-/- + Uninfected
CD300f-/- + R. typhi
CD300f-/- + Uninfected
CD300f-/- + R. rickettsii
CD300d-/- + Uninfected
CD300d-/- + R. typhi
CD300d-/- + Uninfected
CD300d-/- + R. rickettsii
C
IL-1β (pg/ml)
IL-1α (pg/ml)
IL-10 (ng/ml)
***
24 h
BMDMΦ WT + Uninfected
BMDMΦ CD300f-/- + Uninfected
BMDMΦ WT + R. typhi
BMDMΦ CD300f-/- + R. typhi
BMDMΦ WT + Uninfected
BMDMΦ CD300f-/- + Uninfected
BMDMΦ WT + R. rickettsii
BMDMΦ CD300f-/- + R. rickettsii
D
BMDMΦ + R. typhi
E
BMDMΦ + R. rickettsii
Time (h)
WT + αIgGs
WT + αIL-1α
WT + αIL-1β
WT + αIL-1α/IL-1β
CD300f-/- + αIgGs
CD300f-/- + αIL-1α
CD300f-/- + αIL-1β
CD300f-/- + αIL-1α/IL-1β